Structure and analgesic properties of layered double hydroxides intercalated with low amounts of ibuprofen

Robson Sousa, Jenny Jouin, Olivier Masson, Fabien Remondiere, Alex Lemarchand, Maggy Colas, Philippe Thomas, Jerônimo Lameira, Gilmara Bastos, Anderson Lima, et al.

Structure and analgesic properties of Layered Double Hydroxides intercalated with low amounts of Ibuprofen

Robson Sousa[1,2], Jenny Jouin[2], Olivier Masson[2*], Fabien Remondiere[2], Alex Lemarchand[2], Maggy Colas[2], Philippe Thomas[2], Jerônimo Lameira[1], Gilmara N. T. Bastos[3], Anderson B. Lima[3], José L. M. Nascimento[4], Marcos Anicete-Santos[1], Waldinei R. Monteiro[1*], Cláudio N. Alves[1]

[1]*Laboratório de Planejamento e Desenvolvimento de Fármacos, Instituto de Ciências Exatas e Naturais, Universidade Federal do Pará, Rua Augusto Corrêa No. 1, CEP: 66075-110 Belém, PA, Brazil.*

[2]*Laboratoire SPCTS, Université de Limoges - CNRS UMR 7315, Centre Européen de la Céramique, 12 rue Atlantis, 87068 Limoges, France.*

[3]*Laboratório de neuroinflamação, Instituto de Ciências Biológicas, Universidade Federal do Pará, Belém, PA, Brazil.*

[4]*Laboratório de Neuroquímica Molecular e Celular, Instituto de Ciências Biológicas, Universidade Federal do Pará, Belém, PA, Brazil.*

ABSTRACT

Ibuprofen-intercalated layered double hydroxides (LDH-IBU) have been successfully synthesized via a co-precipitation method with a nominal $[Al^{3+}]/[Mg^{2+}]$ ratio of 0.5 and a variable molar IBU/($[Al^{3+}]+[Mg^{2+}]$) ratio of 0, 0.15, 0.18, 0.24, 0.36 and 0.72. After an accurate determination of the composition, the nature of the intercalated species and the effective intercalation yield from NO_3^- to IBU, it is shown that the synthesis route used allows a good control of the quantity of intercalated IBU within the LDH framework. This results in different samples with full or partial IBU intercalation in the interlayer space in exchange of nitrate anions. The analysis of the X-ray diffraction basal reflections reveals that the intercalation of IBU in the framework only increases the basal distances with no alteration of the brucite-type layers. Also, a computational study used to model the positions and shapes of the basal reflections showed that the structure of the non-fully intercalated compounds follows a random

interstratification scheme. Finally three samples ranging from slightly to fully IBU-intercalated galleries were selected for preliminary *in vivo* assays. These tests showed a strong tendency that after 24 hours the low yield of IBU-intercalated compounds are almost as efficient as the fully intercalated sample.

Keywords: Layered Double Hydroxide, Mg-Al hydrotalcite, Ibuprofen, Intercalation process, Structure characterisation, Co-precipitiation

*Corresponding authors: olivier.masson@unilim.fr

waldinei@ufpa.br

1. Introduction

Layered Double Hydroxides (LDH) compounds represent a huge family of materials also known as anionic clays [1, 2]. They exhibit a lamellar structure based on softly bonded brucite-type layers [$Mg(OH_2)$] composed of edge-linked $Mg(OH)_6$ octahedra [3]. Substitutions of Mg^{2+} by other metals are possible; and in the case of some M^{3+}, it leads to positively charged brucite-type layers, which then can be compensated by negative charges in the interlayer space. Different anions can be intercalated, typically CO_3^{2-}, SO_4^{2-}, OH^-, F^-, Cl^-, Br^- or NO_3^-, with a decreasing affinity for the interlayer spacing in this list [4]. Among the most promising LDH materials in this field are the aluminium-substituted magnesium compounds, referenced as Mg,Al-LDH [1, 2, 5, 6]. Their general formula is $[Mg_{1-x}^{2+}Al_x^{3+}(OH)_2]^{x+}(A^{n-})_{x/n}.zH_2O$ [1, 2, 7], where A^{n-} are interlayer anions, often carbonates and nitrates, which compensate for the positively charged hydroxide brucite-type layers, x refers to the molar fraction $Al^{3+}/(Mg^{2+}+Al^{3+})$ usually ranging between 0.2 and 0.4 [1, 2], and z is the amount of hydration water molecules.

Generally, LDH are of great interest in materials science and technology because of their versatile structures, their intercalation properties [8] and their wide range of applications [1, 2, 9] such as catalysis [10, 11], photochemistry [12, 13] and adsorbents [14, 15]. More recently, they have been extensively studied as anionic drugs carriers [16] due to their good ion-exchange properties, low cytotoxicity, high biocompatibility and low cost [17]. For this application, the drug is intercalated into the LDH host framework in order to improve its pharmacological activity and duration of action [5, 16].

Numerous works in the literature have been devoted to the synthesis of LDH-IBU hybrids by various methods [9, 18, 19, 20, 21] and the study of drug release properties. Among these, the co-precipitation method [22], based on the mixing of metal salts at a constant pH, is the most widely applied due to its relative ease of use and good control over the stoichiometry of the final product.

Since the year 2000, many molecules with biological activity presenting anionic form have been successfully intercalated into Mg,Al-LDH [1, 23] This is notably the case for ibuprofen (α-methyl-4-(2-methylpropyl) benzene-acetic acid), a non-steroidal antiinflammatory drug (NSAID) widely used for the treatment of rheumatoid arthritis and osteoarthritis [24]. Although efficient, this drug has a short half-life and side effects, such as gastric irritability and risk of central nervous system ailment. Therefore, the intercalation of ibuprofen into LDH can contribute for reducing the side effects of this drug, prolonging its half-life and consequently its analgesic effect [24]. However, few works have been reported concerning the *in vivo* assays [6] and, to the best of our knowledge, there are no studies dealing with the behaviour of the LDH-IBU complex at small intercalation yield in particular regarding their structure and analgesic activity. For example, it is not clear how to obtain a long term analgesic activity using LDH-IBU, whether LDH galleries must be fully or partially filled of IBU in order to achieve the best drug release control. In addition, it is not clear whether the structure of slightly intercalated compounds is characterised by staging phenomena or random interstratification.

In this study, we report the synthesis, followed by a chemical and structural characterization of LDH intercalated with ibuprofen (LDH-IBU) using variable molar ratio IBU/([Al^{3+}]+[Mg^{2+}]) of 0, 0.15, 0.18, 0.24, 0.36 and 0.72. We also report a structural analysis of the intercalation mechanism in these different compositions.

Moreover, preliminary *in vivo* assays were performed for three samples ranging from slightly to fully IBU-intercalated complex galleries in order to explore the long term analgesic effects of LDH-IBU.

2. Experimental

2.1. Synthesis

Ibuprofen (labeled IBU hereinafter, Sigma-Aldrich Brazil Ltds 98%), $Mg(NO_3)_2.6H_2O$ (Sigma-Aldrich, 98%), $Al(NO_3)_3.9H_2O$ (Sigma-Aldrich, 98%), NaOH (Sigma-Aldrich, 98%), CH_3CH_2OH (Alfa Aesar, 94-96%) were used as starting reagents. Deionized water (ELGA Purelab) was decarbonated prior to the synthesis in order to avoid the intercalation of CO_3^{2-} in the samples, and phosphate buffer pH = 7.00 ± 0.02 was purchased from Sigma-Aldrich.

The co-precipitation strategy [22, 25] was used to synthesize both pure LDH ($LDH\text{-}NO_3$) and ibuprofen intercalated LDH (LDH-IBU) samples. The cationic molar ratio $[Al^{3+}]/[Mg^{2+}]$ was set to 0.5 for all samples and the $IBU/([Al^{3+}]+[Mg^{2+}])$ nominal molar ratios were 0; 0.15; 0.18; 0.24; 0.36; 0.72 respectively labeled $LDH\text{-}NO_3$, LDH-IBU(10:1); LDH-IBU(8:1); LDH-IBU(6:1); LDH-IBU(4:1); LDH-IBU(2:1).

The $Mg(NO_3)_2.6H_2O$ and $Al(NO_3)_3.9H_2O$ salts dissolved in water were slowly added to a three-neck flask containing aqueous ethanol solution (50 vol.%) with or without dissolved drug. To ensure the dissolution of IBU, the pH of the aqueous ethanol solution was adjusted to 10.0 using a 2.0M NaOH solution. The addition was performed at room temperature under vigorous stirring and N_2 gas flow to avoid carbonate contamination. During the procedure the value of the pH was maintained by continuous addition of the NaOH solution. The resulting suspension of LDH-IBU was kept under

reflux conditions at 80 ºC for 24 h. The solid was then isolated by centrifugation and washed thoroughly three times with aqueous ethanol solution (50 vol.%), and finally dried for 24 h at 60 °C.

2.2. Sample characterization

The phase purity assessment and the structural characterisation of the sample were performed by X-ray diffraction (XRD) and Raman and Fourier transform infrared (FTIR) spectroscopies. The chemical and elemental compositions were determined using inductively coupled plasma (ICP), coupled thermogravimetry and mass spectroscopy (TG/MS), and UV-visible spectroscopies. The morphology of the powders was characterized by field-emission scanning electron microscopy (FE-SEM).

The XRD diagrams of all the samples were collected from 1 to 80° (2θ) with a step of 0.014° and an effective acquisition time of 2.31s per step using a Bruker D8 Advance diffractometer with Bragg-Brentano geometry and LynxEye PSD detector and monochromatic CuKα_1 radiation. The basal spacing values were obtained by performing pattern decompositions using the Peakoc software [26] with a split pseudo-Voigt function [27] to fit the experimental profiles. The structural characterisation of the intercalation of IBU into LDH was performed by analysing the profile shape and positions of the basal reflections using a home-made program written in Python language [28] (see section 3.2.). Micrographs of the powder morphologies were obtained thanks to a JEOL JEM 6700 FE-SEM with at an accelerating voltage of 5.0 kV. Raman spectra were recorded on a Jobin Yvon/Horiba (T6400) spectrophotometer on raw powder samples using excitation wavelength of 514 nm, exposure time of 10 s, power 3 mW, lens x50LWD. FTIR spectra of the samples pressed in KBr were scanned (400 to 4000 cm^{-1}) on a Thermofisher (Nicolet 6700) spectrophotometer with a

resolution of 4 cm^{-1}. Each spectrum is the average of 32 successive scans. ICP measurements were accomplished using a Perkin Elmer Optima 8300 instrument to determine the relative amount $[Al^{3+}]/[Mg^{2+}]$ on powders calcined at 1000°C for 30 minutes. The thermogravimetric analyses were performed on a Netzsch instrument (model STA 449F3, Germany). The analyses were carried out from 25°C to 1000°C at a heating rate of 10°C/min in flowing argon gas (20 mL/min). The titration of IBU released from the intercalated samples was determined after dissolution of the LDH host using a Shimadzu UV-2600 model UV-Vis spectroscope. The following method was used: 5 mg of LDHs-IBU sample was dissolved in 2 mL of ethanol, 1 mL of 0.1M HCl solution and successive dilution with phosphate buffer at pH 7.00 ± 0.02 in a 10 mL volumetric flask. The concentration of IBU in the resulting solutions was determined by measuring the absorbance at λ_{max} = 264 nm and was calculated by regression analysis according to a calibration curve obtained from a series of standard solutions of pure IBU.

2.3. *In vivo* assays

The *in vivo* assays of the analgesic activity of LDH-IBU samples were performed using 6 to 8 week-old male Swiss mice with an average weight of 20-25 grams obtained from colonies maintained at the Evandro Chagas Institute (Belém, Brazil). The mice were housed in groups of 5 under environmentally controlled conditions: 25 ± 2°C under a 12h/12h light/dark cycle. Food and water were supplied *ad libitum*. The handling and use of the animals were in accordance with the institutional guidelines (CEPAE 124-13).

The analgesic activities of LDH-IBU(10:1), LDH-IBU(6:1) and LDH-IBU(4:1) samples were evaluated using the acetic acid-induced writhing method as described by

Koster *et al.* and de Lima *et al.* [29, 30]. For the test, a group of 5 mice was treated by oral administration with 200 mg/kg (mass of sample per mice weight) of LDH-IBU powder, employing the samples LDH-IBU (4:1), LDH-IBU (6:1) and LDH-IBU (10:1). For comparison, the mice were also treated in the same way with pure LDH-NO_3 (200 mg/kg), ibuprofen (200 mg/kg) and vehicle (saline plus 1% Dimethyl sulfoxide) at equivalent volumes. The writhing was induced by intra-peritoneal injection of 0.6% of acetic acid to the mice. After 24 hours, the mice were observed and the number of writhing was counted for 30 min [29]. The contractions of the abdomen, elongation of the body, twisting of the trunk and/or pelvis ending with the extension of the limbs were considered as complete writhing. The number of writhing, expressed as mean ± S.E.M., were compared using an analysis of variance (ANOVA) followed by a Student-Newman-Keuls test [31], and values were considered significantly different when $P < 0.05$.

3. Results and discussion

3.1. Samples characterization

The XRD patterns of the synthesised samples are reported in Figure 1. They all correspond to single phase compounds with no evidence of crystallised impurities such as sodium nitrate or recrystallized ibuprofen. The pattern of the ibuprofen-free (i.e. non-intercalated) sample (LDH-NO_3) is typical of the 3R1 polytype of the hydrotalcite structure with c ~ 24 Å corresponding to the stacking of 3 brucite layers [32]. The basal spacing, given by the 003 reflection, is about 8.70 Å, which corresponds to typical values found with intercalated nitrate ions [33, 34] The 01ℓ reflections (*i.e.* 012, 015 and 018) are clearly asymmetric toward high angles, indicating the presence of stacking faults in the brucite layers stacking sequence. The pattern of the sample with the highest

nominal IBU content is clearly different. Its first and highest peak is located at lower angles (~ 4° 2θ), indicating a much larger basal spacing of about 22.2 Å. This is perfectly consistent with an effective intercalation of IBU anions into the brucite interlayer spaces as described in previous studies [20, 24, 35, 36]. The five following diffraction lines correspond to the successive integral orders of the first reflection, i.e. with integer d-spacing ratios. Note that for the sake of comparison with the ibuprofen-free sample, we used the same indexation of the first line (no experimental fact at this level of analysis suggests 003 instead of 001). Now, focusing on the samples with intermediate nominal IBU contents we can clearly observe a smooth evolution of the corresponding XRD patterns. When increasing the amount of IBU, the 003 reflection seems to split into two reflections. At first these two reflections are overlapped but then progressively separate to finally correspond to the 006 and 009 reflections of the sample with highest IBU content. In addition, a low intensity peak appears at very low angle (~2.5° 2θ) and progressively increases in intensity and slightly shifts toward higher angles to finally correspond to the 003 reflection of the sample with the highest IBU content. This clearly does not correspond to a continuous increase of the interlayer spacing. Instead, the basal reflections now form a non-integral reflection series (i.e. with non-rational d-spacing ratios), typical of interstratification phenomena. This latter is induced by the progressive intercalation of IBU into the interlayer spaces and will be discussed in details in the intercalation process section. The only part of the diagram that does not undergo significant change corresponds to the 110 reflection, which appears at the same position (~60.5° 2θ) for all the samples, indicating that the structure of the brucite layers is almost unaffected by the addition of IBU.

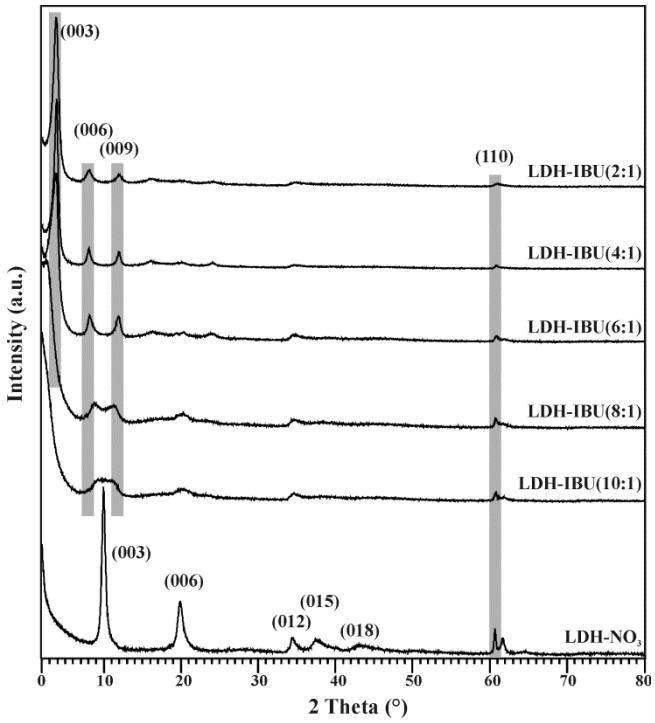

Figure 1: XRD diagrams of LDH-NO3 and LDH-IBU samples.

The FE-SEM micrographs of the samples are shown in Figure 2. They are very similar whatever the initial nominal content of IBU in the reaction mixture. The image suggests an aggregated sheet-like morphology expected for hydrotalcite-like compounds [24] characterized by a particle size of about 100 nm and a thickness of a few nanometres. This thickness indicates that the particles are composed of a small number of layers (typically less than 10). They are slightly larger that LDH-Cl^- hydrotalcites obtained by mecanochemistry and hydrothermal synthesis [37] but stay within the same range and aggregation state.

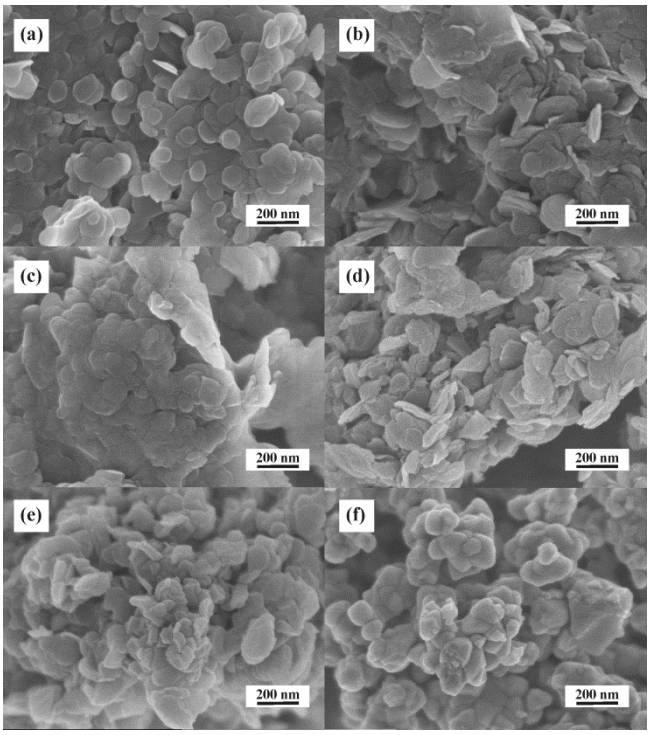

Figure 2: FE-SEM images of (a) LDH-NO_3, (b)LDH-IBU(10:1), (c)LDH-IBU(8:1), (d)LDH-IBU(6:1), (e)LDH-IBU(4:1), (f)LDH-IBU(2:1).

The Raman spectra of all the samples are shown in Figure 3(a). In the LDH-NO_3 sample, one can observe a band related to the nitrate (symmetry D_{3h}) at 1062 cm^{-1} as reported by Kloprogge *et al.* [38, 39]. The measured IBU spectrum confirms that the drug is pure and matches well with the full indexation proposed by Vueba *et al.* [40] Based on these previous measurements, the analysis confirms the successful intercalation of IBU in the hosts as evidenced by the structural asymmetric vibrations of CH_3 at 2955 cm^{-1}, CH_3 symmetric stretching mode at 2867 cm^{-1} and CH_2 asymmetric stretching at 2912 cm^{-1}, all corresponding to IBU. Moreover, the band related to the nitrate anion vanishes for samples with nominal IBU ratio of at least 0.36 (LDH-IBU(4:1)). Finally, two distinct and well defined bands can be seen at 558 cm^{-1} and

722 cm^{-1}. They are attributed to M-OH bonds and are not modified nor shifted during the intercalation process, thus attesting no drastic change in the brucite-type layers.

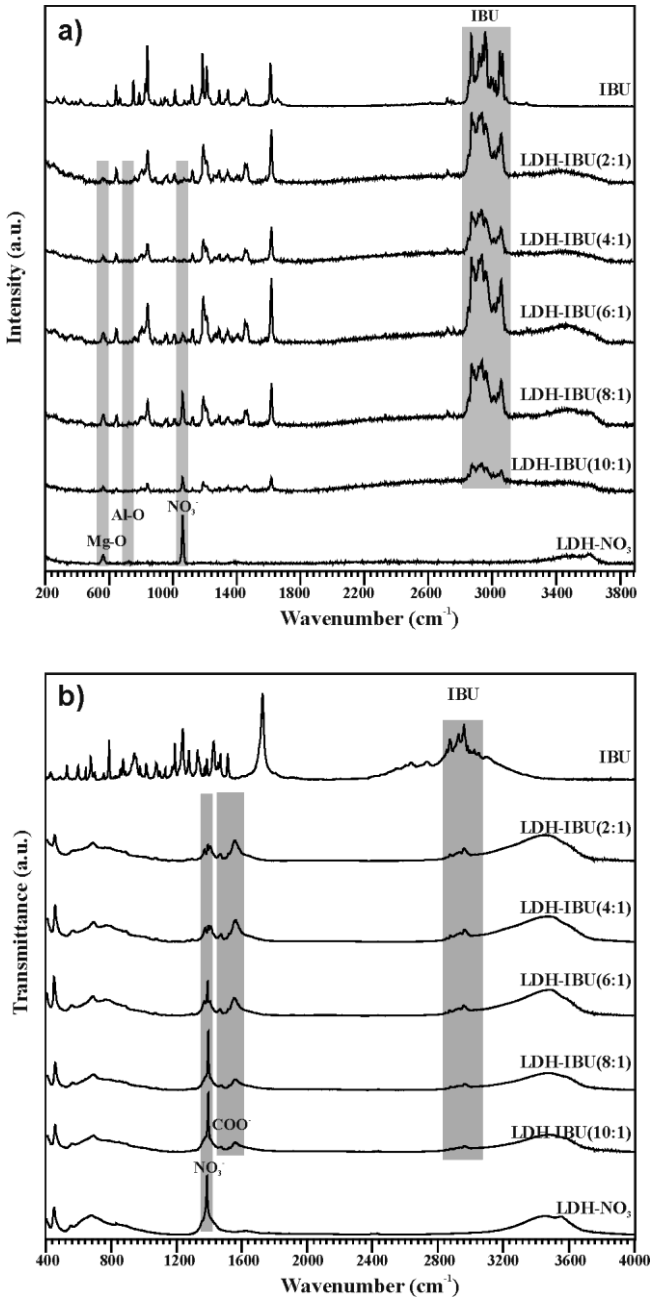

Figure 3: (a) Raman spectra (b) FTIR spectra of IBU, LDH-NO_3, LDH-IBU(2:1), LDH-IBU(4:1), LDH-IBU(6:1), LDH-IBU(8:1), LDH-IBU(10:1).

The measured FTIR spectra of raw and intercalated LDH, shown in Figure 3(b), are in agreement with the previous observations issued from Raman. Indeed the presence of NO_3^- is evidenced by a sharp characteristic peak at 1385 cm^{-1}, unambiguously assigned to its ν_3 vibrational mode [41] for all the samples below the IBU ratio of 0.36. All vibrational modes of raw IBU spectra match with a previous assignment proposed by Vueba *et al.* [40] In the case of intercalated compounds, specific bands are observed at 1400 cm^{-1} and 1550-1554 cm^{-1}. They correspond respectively to the symmetric and asymmetric vibration of carbonyl bond in the case of a carboxylate function according to Mohanembe *et al.* [42]. This feature clearly indicates the deprotanated nature of the intercalated IBU as compared to the raw one.

The results regarding the actual chemical composition of the samples are gathered in Table 1. The cationic ratio obtained from ICP on the calcined samples allowed calculating the composition and the positive charge of the brucite layer. As we can see in Table 1, there is a slight deviation with respect to the target values. This indicates a minor loss of Al^{3+} probably due to the possible formation of aluminium complex $[Al(OH)_4]^-$ for such alkaline conditions [43] and its elimination during the washing step. The amount of intercalated IBU and water of hydration per formula unit were obtained using the weight percent of intercalated IBU determined using UV-Vis spectroscopy analysis and the total weight loss measured by TG analysis (Table 1). For the calculation, it was assumed that one ibuprofenate ion substitutes for one nitrate ion in the intercalated compounds and that the total weight loss is due to the removal of interlayer water molecules, the dehydroxylation of the brucite-type layers and the decomposition of the interlayer anions (NO_3^-, IBU^-). This latter assumption is supported by the mass spectroscopy data and the shape of the TG curves characterized by two major weight losses as already observed by other authors [21, 34] (TG data are not

shown here but can be provided on request). As we can see in Table 1, the hydration yield is about 0.5 water molecules per formula unit, with slight variations from one sample to another.

Table 1: IBU/([Al^{3+}]+[Mg^{2+}]) nominal molar ratio, cationic ratio weight% of IBU content, total weight losses at 800°C and chemical compositions of the synthesized samples.

Sample	Nominal molar IBU/([Al^{3+}] + [Mg^{2+}]) ratio	Cationic ratio [Al^{3+}]/[Mg^{2+}] #	Weight % of IBU ϰ	Total weight loss ‡	Average chemical composition
LDH-NO_3	0	0.48	0.0%	48.81%	$[Mg_{0.68}Al_{0.32}(OH)_2]^{0.32+}[(NO_3)_{0.32},0.36H_2O]^{0.32-}$
LDH-IBU(10:1)	0.15	0.47	22.5%	59.11%	$[Mg_{0.68}Al_{0.32}(OH)_2]^{0.32+}[(NO_3)_{0.19}IBU_{0.13},0.48H_2O]^{0.32-}$
LDH-IBU(8:1)	0.18	0.47	27.7%	61.34%	$[Mg_{0.68}Al_{0.32}(OH)_2]^{0.32+}[(NO_3)_{0.15}IBU_{0.17},0.54H_2O]^{0.32-}$
LDH-IBU(6:1)	0.24	0.48	35.0%	64.87%	$[Mg_{0.68}Al_{0.32}(OH)_2]^{0.32+}[(NO_3)_{0.08}IBU_{0.24},0.62H_2O]^{0.32-}$
LDH-IBU(4:1)	0.36	0.49	47.2%	67.34%	$[Mg_{0.67}Al_{0.33}(OH)_2]^{0.33+}[(NO_3)_{0.01}IBU_{0.32},0.52H_2O]^{0.33-}$
LDH-IBU(2:1)	0.72	0.47	46.5%	66.96%	$[Mg_{0.68}Al_{0.32}(OH)_2]^{0.32+}[(NO_3)_{0.01}IBU_{0.31},0.49H_2O]^{0.32-}$

based on ICP measurements, ϰ based on UV-Vis titration, ‡ based on TG analyses

The intercalation yields were finally deduced from the sample chemical compositions. They are plotted as a function of the nominal IBU ratio in Figure 4. We can clearly distinguish two evolution domains. From 0 up to about 0.34, the content of intercalated IBU increases linearly, while above 0.34 it is constant and equal to a maximum value of about 94%. This clearly indicates that saturation of the interlayer galleries is reached above a nominal IBU ratio of 0.34. This also demonstrates that the

synthesis route used in this work makes it possible to simply and precisely control the quantity of intercalated IBU within the LDH framework.

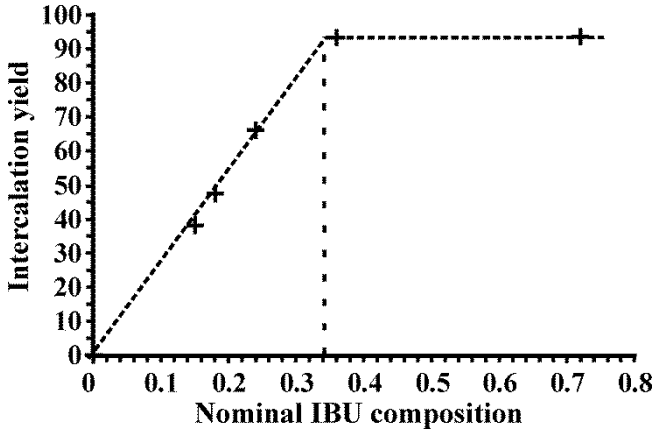

Figure 4: Evolution of the IBU intercalation yield as a function of nominal IBU ratio determined by ICP, TG and UV-Vis methods.

3.2. Intercalation process

As discussed above, the changes in the experimental XRD patterns observed on our samples with increasing the amount of intercalated IBU do not correspond to a continuous increase of the basal spacing. They instead suggest that there are only a limited number of definite interlayer spacings, corresponding to gallery filled by either the intercalant NO_3^- or IBU^- anions or both (the gallery being partially or fully filled), which are mixed and distributed with some degrees of randomness. This phenomenon is known as interstratification or interlayering and can proceed via various schemes [44] including: random interstratification (Hendricks-Teller scheme), partial ordering, staging (i.e. regular alternation of interlayers) and segregation (i.e. the intercalant anions are clustered into completely discrete domains). It has been observed for a long time in

clay materials [44, 45] , including LDH [46], but its characterisation in the present case of LDH-IBU compounds has received only limited attention, with only one reference in the last years [36]. In order to clarify this point and access the proportions of layers filled by IBU^- or NO_3^- ions and their ordering sequence, we analysed the basal reflections of the XRD patterns in terms of position and profile width and shape. Different methods for tackling this problem can be found in literature [45, 47]. Here, we considered the following simplified model. The LDH-IBU crystallites were modelled as a stacking of identical layers, i.e. with identical structure factor, separated by only two possible interlayer spacings. It was assumed that IBU^- anions do not induce significant distortions of the relatively rigid brucite layers. As each brucite layer consists of two adjacent hexagonal closed-packed arrays of hydroxide ions with Mg^{2+}/Al^{3+} cations filling all the octahedral spaces between them, it was modelled by 3 equidistant layers of identical electronic density. In addition, the structure of the interlayers being not well-known and the electronic density being low, their structure factors were simply neglected. This simplification only affects the relative peak intensities but not the peak positions and shapes. Finally, statistical fluctuations of the interlayers spacing and the number of layers per crystallite were considered. For this latter, the well-suited Poisson distribution was used. According to this simplified model, the scattered intensity corresponding to the basal reflections can be written as (exclusive of Lorentz polarization and other geometric or instrumental effects) [48]:

$$I(s) = F^2 \times \left\{ \overline{N} + 2 \times \sum_{n=1}^{N_{max}-1} \left(\sum_{N=n+1}^{N_{max}} p(n)(N-n) \right) \times e^{-2\pi^2 n \delta s^2} \times \langle \cos[2\pi d(n) s] \rangle \right\}$$

, where $s=2\sin(\theta)/\lambda$ is the scattering vector length with wavelength λ and scattering angle 2θ, F is the layer structure factor, $\overline{N}$ and N_{max} are the average number and

maximum number of layers per crystallite respectively, *p(n)* the Poisson probability mass function, δ the variance of statistical fluctuations of the interlayers spacing, *d(n)* the distance between two n^{th}-nearest neighbour layers. The average phase term in brackets was evaluated using the recursive algorithm for frequency factors calculation proposed by Reynolds [49] for two types of interlayers and nearest-neighbour correlations (i.e. Reichweite parameter equal to 1). The calculations were performed using a home-made program written in Python language [28].The input parameters were $\overline{N}$, δ, the two interlayer spacings, d_A and d_B, for interlayer filled with NO_3^- and IBU^- ions respectively, the percentage, P_B, of interlayer filled with IBU^- ions, and the junction probability, P_{BB}, of interlayer filled with IBU^- ions following interlayer filled with IBU^- ions as well.

Different cases of interstratification schemes, ranging from random to ordered, were tested. The best agreements between calculated and experimental data were systematically obtained for the random interstratification model. They are plotted in Figure 5a-d for samples LDH-IBU(4:1), (6:1), (8:1) and (10:1) respectively. The calculation obtained for the (8:1) sample (i.e. with an intercalation yield of about 50%) with a 2^{nd}-stage (i.e. perfectly ordered) model is also plotted for comparison. The random model clearly gives the best agreement. All the calculations were performed with $\overline{N}$ = 8, δ = 0.3 $Å^2$, d_A = 8.5 Å, d_B= 22.0 Å, which corresponds to LDH-IBU particles of about 10-15 nm in thickness. Only the proportions of layers filled with IBU^- were required to vary (as well as the junction probabilities accordingly). The obtained values are 90%, 70%, 40% and 25% for the (4:1), (6:1), (8:1) and (10:1) LDH-IBU samples respectively.

As we can see from Figure 5, the agreement between the experimental and calculated positions and profile shapes of the basal reflections of the four samples is rather good. In addition, the obtained proportions of layers filled with IBU^- anions are overall consistent (even if we can notice larger discrepancies with the lowest values) with the measured intercalation yields (94%, 66%, 48% and 37%) given in the previous section. All these results suggest that the synthesis method used in this work induces a random filling of the LDH galleries. No staging was evidenced.

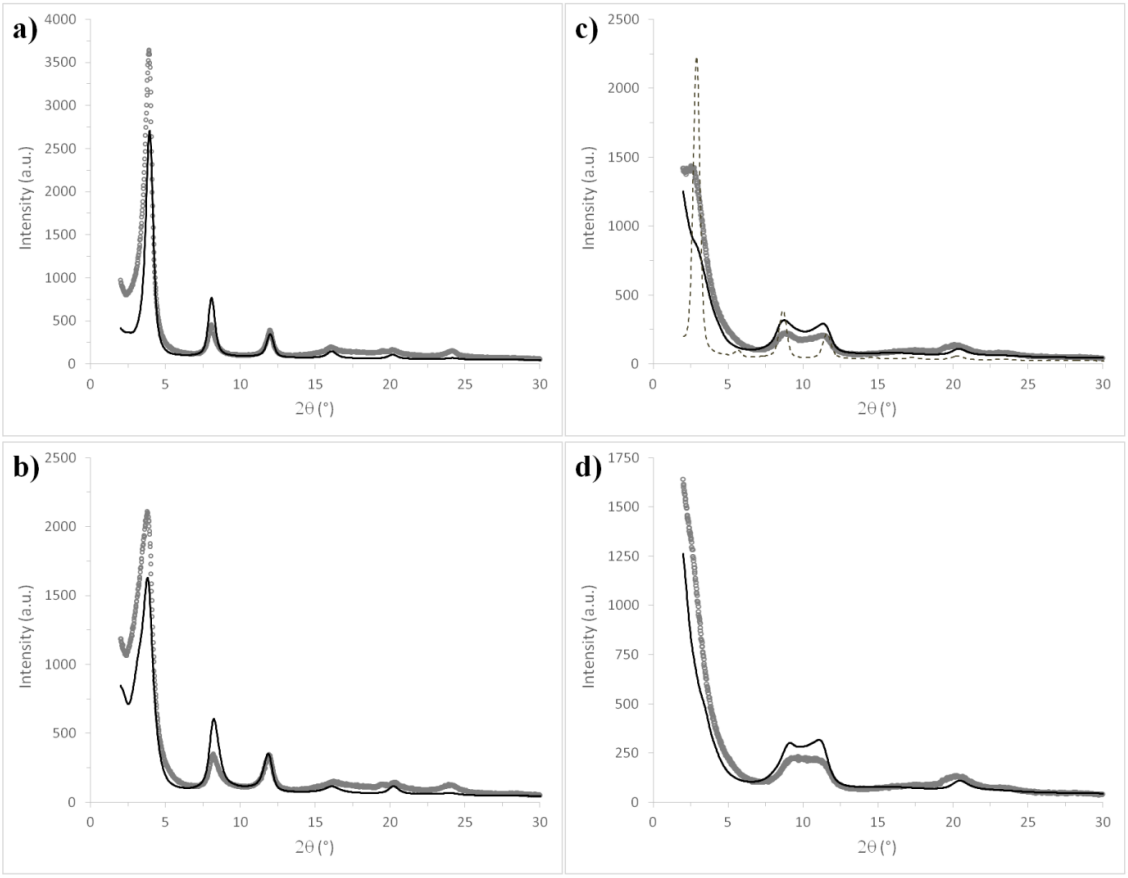

Figure 5: Comparison between the experimental patterns of the LDH-IBU(4:1) (a), LDH-IBU(6:1) (b), LDH-IBU(8:1) (c) and LDH-IBU(10:1) (d) samples and the patterns calculated with a random interstratification model. For LDH-IBU(8:1) (c), calculation obtained with a 2^{nd}-stage model is also plotted for comparison. All calculations were performed with the following parameters: $\bar{N}$ = 8, δ = 0.3 Å^2, d_A = 8.5 Å, d_B= 22.0 Å.

3.3. The antinociceptive activity

The results of the preliminary *in vivo* tests of the analgesic activity are reported in Figure 6. We can see that only the LDH-IBU samples present antinociceptive activity after 24 hours. In contrast, the number of writhing measured for mice treated with free IBU is statistically equal to that measured with vehicle or LDH alone, indicating that free IBU has no effect after 24 hours. In addition, the decrease of writhing observed for mice treated with LDH-IBU samples is significant, being larger than 60% even for the sample with lowest intercalation yield. This result suggest that the long term analgesic effects is observed only for LDH-IBU complexes, in other words, the intercalation of IBU into LDH has a large delaying effect on its release within the mice body and that IBU is still efficiently present in mice after 24 hours.

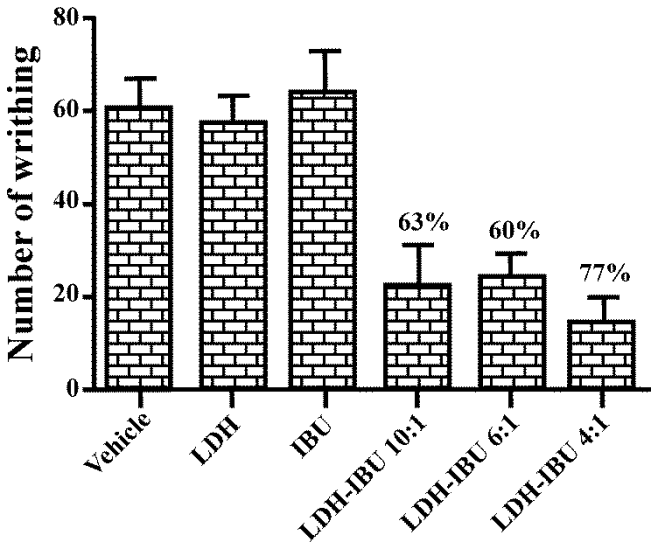

Figure 6: Bar graph representing the number of writhing, expressed as Mean±S.E.M., measured 24 hours after the beginning of nociception induced by injection of acetic acid for mice treated with LDH-IBU(10:1), LDH-IBU(6:1), LDH-IBU(4:1), LDH-NO_3, IBU, and vehicle. The numbers above the bars correspond to the percent decrease of the number of writhing with respect to that obtained with vehicle alone.

Curiously, there is no significant statistical difference between the analgesic effects of the three LDH-IBU samples despite their very different intercalation yields. In particular, the 40% intercalated LDH-IBU(10:1) sample is almost as efficient as the fully intercalated LDH-IBU(4:1) sample after 24 hours. This fact is particularly interesting as it suggests that achieving a long term antinociceptive activity does not necessarily requires a large amount of intercalated drug and that low quantity of IBU intercalated into LDH can also provide an efficient biological activity. It is certainly related to the difference of IBU release kinetics between the fully and non-fully intercalated samples, in particular at short time after administering LDH-IBU and its precise understanding thus requires further investigation on the kinetics behaviours of the samples. This, in turn, is likely related to the structure of the intercalated compounds, in particular their random interstratification, as this latter can affect the stability (e.g. with respect to defoliation) of the LDH-IBU crystallites within the body.

4. Conclusion

The co-precipitation method presented in this study allows obtaining pure ibuprofen-intercalated layered double hydroxides (LDH-IBU) compounds with almost constant LDH framework composition and precisely controllable intercalated IBU content. The cationic nominal ratio of these compounds which was set to $[Al^{3+}]/[Mg^{2+}]=0.5$ was well respected in the final products. The quantity of intercalated IBU increased linearly in the synthesized samples, until it reached its maximum intercalation yield of about 94%. The spectroscopic studies confirmed that only the unprotonated form of IBU intercalates within the basal spacing. The structural study of the LDH-IBU compounds showed that the intercalation of IBU only affects the interlayer area without major modification of the brucite-type layers. Furthermore, a

computational modelling of the shapes and positions of the basal reflections showed that intercalation proceeds via random interstratification, without staging phenomena. The *in vivo* assays performed on male Swiss mice revealed a significant increase of the antinociceptive effect of the LDH-IBU samples after 24 hours with respect to raw IBU. More importantly, the tests also reveal that the low IBU-intercalated compounds are almost as efficient as the fully intercalated sample. This latter result may have non negligible impact on the optimal way of using LDH as a drug carrier.

Acknowledgements

The work was partially supported by the Brazilian agencies MCTI, CNPq, CAPES, FAPESP, FAPESPA and PROPESP/UFPA. The work was also partially supported by the French CAPES-COFECUB program (Ph-C 780-13). The authors are grateful to J. Cornette, A. Meguekam-Sado and R. Mayet for IR-Raman, SEM and XRD measurements.

References

1 V. Rives (ed.), *Layered Double Hydroxides: Present and Future*. Nova Science Publishers, New York (2001).

2 X. Duan and D.G. Evans, *Layered Double Hydroxides: in Structure and Bondings*, vol. 119, eds Springer-Verlag, Berlin (2006).

3 D. G. Evans et R. C. T. Slade, Structural Aspects of Layered Double Hydroxides, in *Layered Double Hydroxides*, X. Duan et D. G. Evans, ed. Springer Berlin Heidelberg, 1-87 (2006).

4 S. Miyata, Anion-Exchange Properties of Hydrotalcite-Like Compounds, *Clays and Clay Minerals* **31(4)**, 305-311 (1983).

5 C. Del Hoyo, Layered Double Hydroxides and Human Health: an Overview, *Appl. Clay Sci.* **36**, 103–121 (2007).

6 M. Del Arco, E. Cebadera, S. Gutierrez, C. Martin, M.J. Montero, V. Rives, J. Rocha and M.A. Sevilla, Mg,Al Layered Double Hydroxides with Intercalated Indomethacin: Synthesis, Characterization, and Pharmacological Study, *J. Pharm. Sci.* **93(6)**, 1649-1658 (2004).

7 G.R. Williams and D. O'Hare, Towards Understanding, Control and Application of Layered Double Hydroxide Chemistry, *J. Mater. Chem.* **16**, 3065-3074 (2006).

8 C. Taviot-Gueho, Y. Feng, A. Faour and F. Leroux, Intercalation Chemistry in a LDH System: Anion Exchange Process and Staging Phenomenon Investigated by Means of Time-Resolved, in Situ X-Ray Diffraction, *Dalton Trans.* **39**, 5994-6005 (2010).

9 H. Abdolmohammad-Zadeh, *Layered double hydroxides: Application to sample preparation methods*, Lap Lambert Academy Publishing, 1-83 (2013).

10 A. Beres, I. Palinko, I. Kiricsi, J.B. Nagy, Y. Kiyozumi and F. Mizukami, Layered Double Hydroxides and Their Pillared Derivatives - Materials for Solid Base Catalysis ; Synthesis and Characterization, *Appl. Catal., A* **182(2)**, 237-247 (1999).

11 A.L. Mckenzie, C.T. Fishel and R.J. Davis, Investigation of the Surface Structure and Basic Properties of Calcined Hydrotalcites, *J. Catal.* **138(2)**, 547-561 (1992).

12 A.W. Musumeci, G.M. Mortimer, M.K. Butler, Z.P. Xu, R.F. Minchin and D.J. Martin, Fluorescent Layered Double Hydroxide Nanoparticles for Biological Studies, *Appl. Clay Sci.* **48(1-2)**, 271-279 (2010).

13 H. Laguna, S. Loera, I.A. Ibarra, E. Lima, M.A. Vera and V. Lara, Azoic Dyes Hosted on Hydrotalcite-Like Compounds: Non-Toxic Hybrid Pigments, *Microporous Mesoporous Mater.* **98(1-3)**, 234-241 (2007).

14 A. Violante, M. Pucci, V. Cozzolino, J. Zhu and M. Pigna, Sorption/Desorption of Arsenate on/from Mg-Al Layered Double Hydroxides: Influence of Phosphate, *J. Colloid Interface Sci.* **333(1)**, 63-70 (2009).

15 K.H. Goh, T.T. Lim, A. Banas and Z. Dong, Sorption Characteristics and Mechanisms of Oxyanions and Oxyhalides Having Different Molecular Properties on Mg/Al Layered Double Hydroxide Nanoparticles, *J. Hazard. Mater.* **179(1-3)**, 818-827 (2010).

16 V. Rives, M. Del Arco and C. Martin, Layered Double Hydroxides as Drug Carriers and for Controlled Release of Non-Steroidal Antiinflammatory Drugs (NSAIDs): a Review, *J. Controlled Release* **169(1-2)**, 28-39 (2013).

17 A.H. Faraji and P. Wipf, Nanoparticles in Cellular Drug Delivery, *Bioorg. Med. Chem.* **17(8)**, 2950-2962 (2009).

18 C.R. Gordijo, C.A. Barbosa, A.M. Da Costa Ferreira, V.R. Constantino and D. De Oliveira Silva, Immobilization of Ibuprofen and Copper-Ibuprofen Drugs on Layered Double Hydroxides, *J. Pharm. Sci.* **94(5)**, 1135-1148 (2005).

19 A.N. Ay, B. Zümreoglu-Karan, A. Temel and V. Rives, Bioinorganic Magnetic Core-Shell Nanocomposites Carrying Antiarthritic Agents: Intercalation of Ibuprofen and Glucuronic Acid into Mg-Al-Layered Double Hydroxides Supported on Magnesium Ferrite, *Inorg. Chem.* **48(18)**, 8871-8877(2009).

20 A.C.S. Alcantara, P. Aranda, M. Darder and E. Ruiz-Hitzky, Bionanocomposites Based on Alginate–Zein/Layered Double Hydroxide Materials as Drug Delivery Systems, *J. Mater. Chem.* **20**, 9495-9504 (2010).

21 X. Lu, L. Meng, H. Li, N. Du, R. Zhang and W. Hou, Facile Fabrication of Ibuprofen–LDH Nanohybrids via a Delamination/Reassembling Process, *Mater. Res. Bull.* **48(4)**, 1512-1517 (2013).

22 F. L. Theiss, G. A. Ayoko and R. L. Frost, Synthesis of Layered Double Hydroxides Containing Mg^{2+}, Zn^{2+}, Ca^{2+} and Al^{3+} Layer Cations by Co-Precipitation Methods-a Review, *Applied Surface Science* **383**, 200-213 (2016).

23 W. Huang, H. Zhang and D. Pan, Study on the Release Behavior and Mechanism by Monitoring the Morphology Changes of the Large-sized Drug-LDH Nanohybrids, *AIChE J.* **57(7)**, 1936-1946 (2011).

24 V. Ambrogi, G. Fardella, G. Grandolini and L. Perioli, Intercalation Compounds of Hydrotalcite-Like Anionic Clays with Antiinflammatory Agents-I. Intercalation and In Vitro Release of Ibuprofen, *Int. J. Pharm. (Amsterdam, Neth.)* **220(1)**, 23–32 (2001).

25 E. Kanezaki, Thermal Behavior of the Hydrotalcite-Like Layered Structure of Mg and Al-Layered Double Hydroxides with Interlayer Carbonate by Means of In Situ Powder HTXRD and DTA/TG, *Solid State Ionics* **106(3-4)**, 279-284 (1998).

26 O. Masson, Peakoc profile fitting program, http://www.esrf.eu/Instrumentation/software/data-analysis (2012).

27 P. Thompson, D.E. Cox and J.B. Hastings, Rietveld Refinement of Debye-Scherrer Synchrotron X-ray Data from Al_2O_3, *J. Appl. Crystallogr.* **20(2)**, 79-83 (1987).

28 O. Masson, PyLDHLineProfile program (2014).

29 R. Koster, M. Anderson and E. De Beer, Acetic Acid for Analgesic Screening, *Fed. Proc.* **18**, 412–416 (1959).

30 A.B. De Lima, M.B. Santana, A.S. Cardoso, J.K.R. Da Silva, J.G.S. Maia, J.C.T. Carvalho and P.J.C. Sousa, Antinociceptive Activity of 1-Nitro-2-Phenylethane, the Main Component of Aniba Canelilla Essential Oil, *Phytomedicine* **16**, 555-559 (2009).

31 H. Abdi and L.J. Williams, *Newman-Keuls Test and Tukey Test*, Encyclopedia of Research design, ed. Neil Salkind, Thousand Oaks, C, (2010).

32 S.J. Mills, A.G. Christy, J-M.R. Génin, T. Kameda and F. Colombo, Nomenclature of the Hydrotalcite Supergroup: Natural Layered Double Hydroxides, *Mineral. Mag.* **76(5)**, 1289-1336 (2012).

33 M. Del Arco, S. Gutiérrez, C. Martín, V. Rives and J. Rocha, Effect of the Mg:Al Ratio on Borate (or Silicate)/Nitrate Exchange in Hydrotalcite, *J. Solid State Chem.* **151(2)**, 272–280 (2000).

34 Z.P. Xu and H.C. Zeng, Decomposition Pathways of Hydrotalcite-Like Compounds $Mg_{1-x}Al_x(OH)_2(NO_3)_x.nH_2O$ as a Continuous Function of Nitrate Anions, *Chem. Mater*. **13(12)**, 4654-4572 (2001).

35 P. Gunawan and R. Xu, Direct Control of Drug Release Behavior from Layered Double Hydroxides Through Particle Interactions, *J. Pharm. Sci*. **97(10)**, 4367-4378 (2008).

36 E. Conterosito, W. Van Beek, L. Palin, G. Croce, L. Perioli, D. Viterbo, G. Gatti and M. Milanesio, Development of a Fast and Clean Intercalation Method for Organic Molecules into Layered Double Hydroxides, *Cryst. Growth Des*. **13(3)**, 1162–1169 (2013).

37 A. Fahami, F.S. Al-Hazmi, A.A. Al-Ghamdi, W.E. Mahmoud and G.W. Beall, Structural Characterization of Chlorine Intercalated Mg-Al Layered Double Hydroxides: a Comparative Study Between Mechanochemistry and Hydrothermal Methods, *J. Alloys Compd*. **683**, 100-107 (2016).

38 R.L. Frost, M.L. Weier and J.T. Kloprogge, Raman Spectroscopy of Some Natural Hydrotalcites with Sulphate and Carbonate in the Interlayer, *J. Raman Spectrosc*. **34(10)**, 760-768 (2003).

39 J.T. Kloprogge, L. Hickey and R.L. Frost, FT-Raman and FT-IR Spectroscopic Study of Synthetic Mg/Zn/Al-Hydrotalcites, *J. Raman Spectrosc*. **35(11)**, 967-974 (2004).

40 M.L. Vueba, M.E. Pina, L.A.E. Batista de Carvalho, Conformational Stability of Ibuprofen: Assessed by DFT Calculations and Optical Vibrational Spectroscopy, *J. Pharm. Sci*. **97(2)**, 845-859 (2008).

41 Z.P. Xu and H.C. Zeng, Abrupt Structural Transformation in Hydrotalcite-like Compounds $Mg_{1-x}Al_x(OH)_2(NO_3)_x.nH_2O$ as a Continuous Function of Nitrate Anions, *J. Phys. Chem. B* **105**, 1743-1749 (2001).

42 L. Mohanambe and S. Vasudevan, Anionic Clays Containing Anti-Inflammatory Drug Molecules: Comparison of Molecular Dynamics Simulation and Measurements, *J. Phys. Chem. B* **109(32)**, 15651-15658 (2005).

43 J.P. Jolivet, J. Livage and M. Henry, *De la solution a l'oxide*, InterEditions, (1994).

44 A. Lerf, Storylines in Intercalation Chemistry, *Dalton Trans.* **43**, 10276 (2014).

45 G. W. Brindley and G. Brown (eds), *Crystal Structures of Clay Minerals and Their X-ray Identification*, Mineralogical Society, London, 249-303 (1980).

46 J. Pisson, C. Taviot-Gueho, Y. Israeli, F. Leroux, P. Munsch, J-P. Itie, V. Briois, N. Morel-Desrosiers and J-P. Besse, Staging of Organic and Inorganic Anions in Layered Double Hydroxides, *J. Phys. Chem. B* **107(35)**, 9243-9248 (2003).

47 M.F. Brigatti and A. Mottana (eds), *Layered mineral structures and their application in advanced technologies*, European Mineralogical Union Notes in Mineralogy, **11** (2011).

48 B.E. Warren, *X-ray diffraction*, Dover Publications Inc., New York, (1990).

49 R.C. Reynolds, Recursive Method for Determining Frequency Factors in Interstratified Clay Diffraction Calculations, *Clays Clay Miner.* **34(2)**, 224-226 (1986).